LA-UR-12-25228
Approved for public release; distribution is unlimited.

Title: Theoretical study of the structure, stability and oxygen reduction activity of ultrathin platinum nanotubes

Author(s): Gonzales, Ivana
Garzon, Fernando H.
Henson, Neil J.

Intended for: 222nd Electrochemical Society Meeting, 2012-10-07/2012-10-12 (Honolulu, Hawaii, United States)

Theoretical Study of the Structure, Stability, and Oxygen Reduction Activity of Ultrathin Platinum Nanotubes

Ivana Matanović, Fernando Garzon, Neil Henson
Physics and Chemistry of Materials
Los Alamos National Laboratory, Los Alamos, USA

222nd ECS, Honolulu, October 2012

abstract

Since the discovery of gold nanowires in 2000 and the later synthesis of similar ultrathin silver and platinum nanotubes, one-dimensional metal nanostructures have attracted a lot of scientific interest due to their peculiar, non-bulk structure and possible applications as nanoelectronic devices. However, platinum is widely used as a catalyst for oxygen reduction reaction (ORR) in proton exchange fuel cells where the chemical reactivity and the durability of the nanomaterial used as a catalyst greatly depends on its size and the structure. In this work we use a plane wave pseudopotential implementation of density functional theory to investigate the structure and stability of number of single and double-wall platinum *(n,m)* nanotubes ranging in diameter from 0.3-2.0 nm in the gas phase and water environment. Furthermore, we are the first to address the possible application of platinum nanotubes as catalyst for oxygen reduction. The change in the catalytic activity with the size and the chirality of the nanotube is studied by calculating equilibrium adsorption potentials for ORR intermediates and by constructing free energy diagrams in the ORR dissociative mechanism network. In addition, the stability of the platinum nanotubes is investigated in the terms of electrochemical dissolution potentials and by determining the most stable state of the material as a function of pH and potential as represented in Pourbaix diagrams.

Our results show that the catalytic activity and the stability towards electrochemical dissolution of platinum nanotubes depend greatly on size and their chirality. Based on the estimated overpotentials for ORR we could conclude that all smaller, ~0.5 nm in diameter single-wall platinum nanotubes consistently show a huge overpotential for oxygen reduction indicating a very poor catalytic activity toward ORR. This is the result of substantial structural changes induced by the adsorption of any intermediate in ORR on these nanotubes. Single-wall *n=m* platinum nanotubes with diameter larger than 1nm have smaller oxygen reduction overpotentials than bulk platinum for up to 180meV and have shown to endure highest cell potentials. However these are still for ~130 meV lower than the dissolution potentials for bulk indicating a possible corrosion problem.

Introduction

- theory plays a crucial role in the design of **new materials** used in heterogeneous catalysis

- **structure of materials (and active sites)**
- **elucidate reaction mechanisms**
- **models for screening of new catalysts** (J. K. Nørskov, *d*-band position – oxygen binding – ORR activity)

oxygen reduction activity

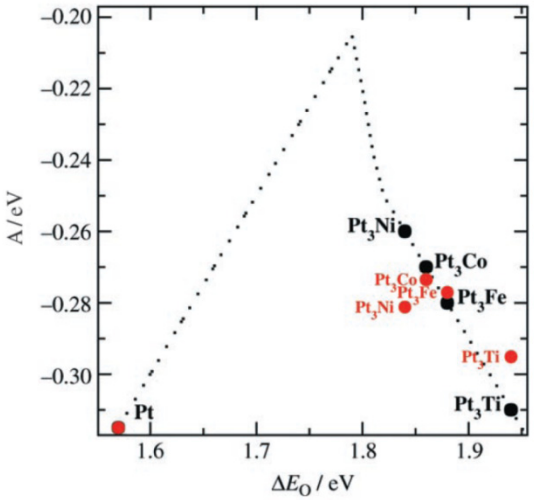

J. K. Nørskov et al. J. Phys, Chem. B, 2004, 108, 17886
V. Stamenkovic et al. Angew. Chem. Int. Ed. 2006, 45, 2987

Motivation

slow kinetics of the oxygen reduction reaction (ORR) in acidic environment

$$O_2(g,1atm) + 4e^- + 4H^+(aq,1M) \rightarrow 2H_2O \quad E^0_{half\_cell} = 1.23V$$

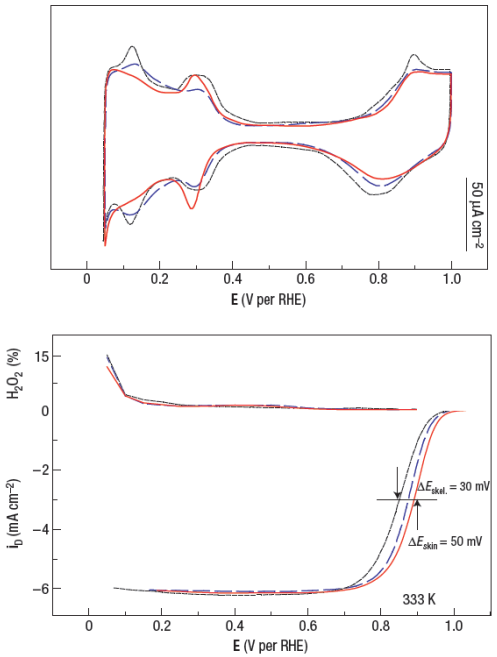

Cyclic voltammograms and polarization curve of ORR on Pt_3Fe

significant cathode overpotential decreases the fuel cell electrical efficiency:

overpotential of 500-600 meV - efficiency of 45-55 % compared to the theoretical thermodynamic efficiency of 93 % at 25℃.

$$\Delta_r G_{cell} = -nF\Delta E_{cell}$$

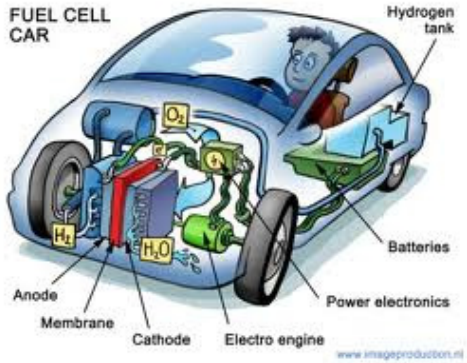

Motivation

Reducing the ORR overpotential / cost:

alloying platinum with platinum group metals

nanostructures
nanotubes and nanoparticles

$Pt_3Ni(111)$ surface

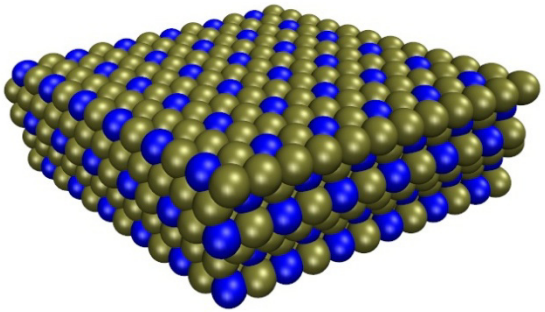

I. Matanovic et al, J. Phys. Chem. C 2011, 115, 10640

(6,6)@(13,13) MWPtNT nanotube
2nm Pt_{201} cluster

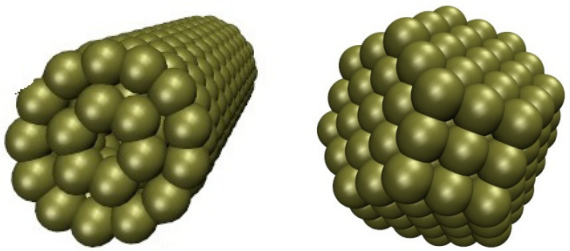

I. Matanovic et al, J. Phys. Chem. C 2012, 116, 16499

metal nanotubes, 2000’

- magic “structure” and conductance - nanoelectronics

- Au, Ag nanotubes less then 2nm thickness have been synthesized by an electron-beam technique in an UHV-TEM

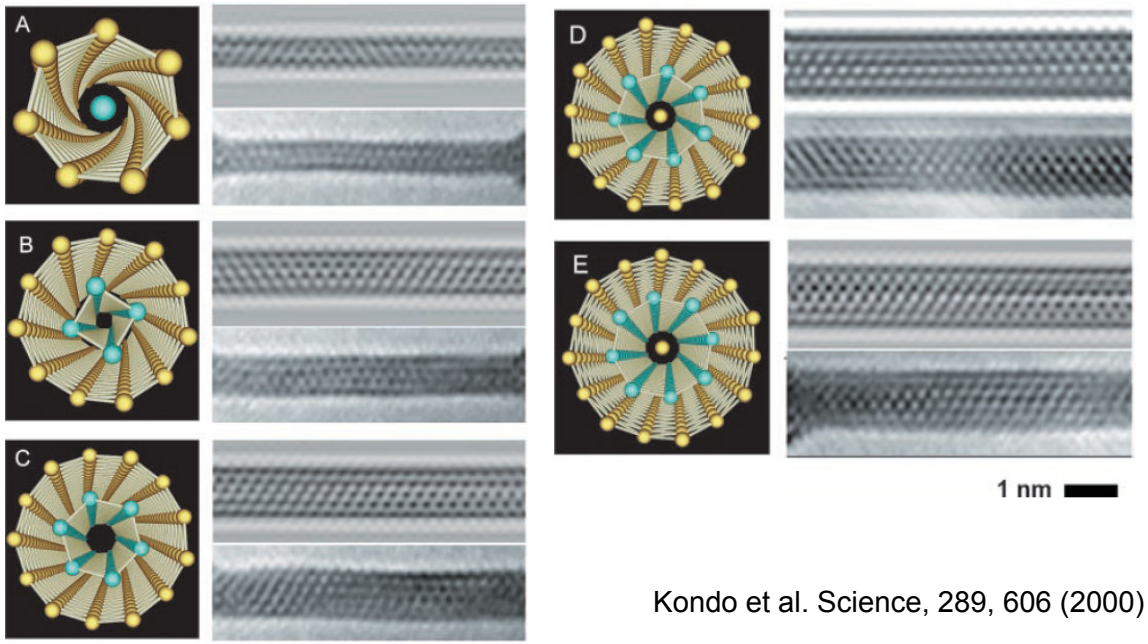

Kondo et al. Science, 289, 606 (2000)

platinum nanotubes, 2002

- Y. Oshima et all. Phys. Rev. B, 65, 121401 (2002)

Pt nanotubes – 1.0 and 0.5 nm in diameter

0.5 nm – six atomic rows coiling around tubes axe

1 nm - 13-6 multishell structure

- C. Koenigsmann, Nano Lett., 10, 2806 (2010)

Pt nanowires with diameter of 1.5 nm

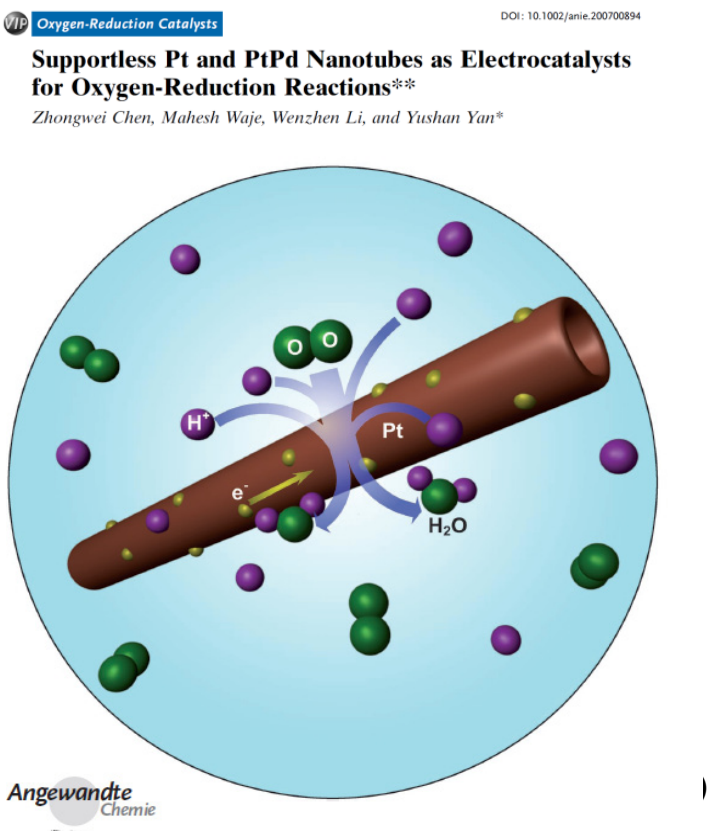

Pt nanotubes

PtNT: Rolling-up Pt(111) sheet to form a tube

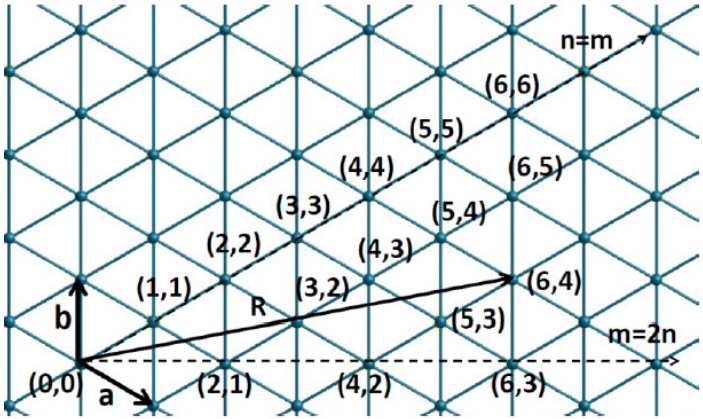

Roll-up

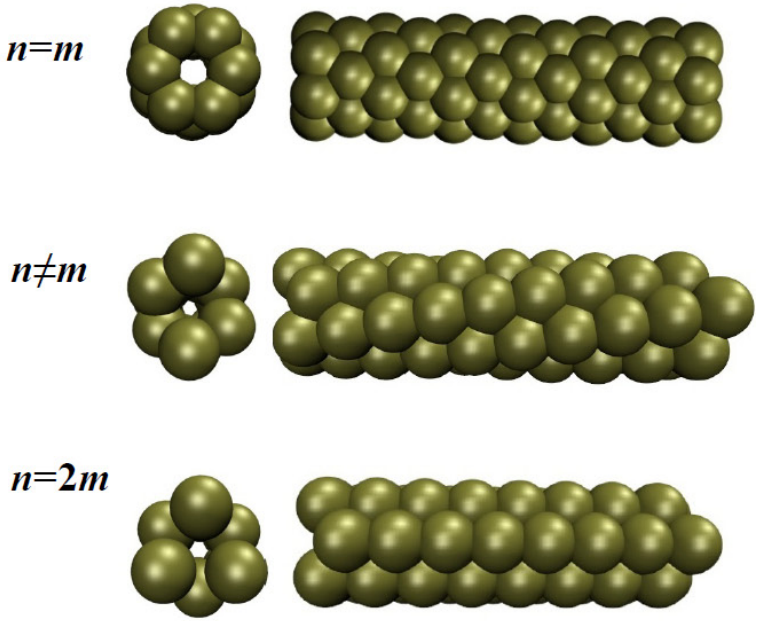

rolling vector: $R = na + mb$

$$r = \frac{\sqrt{2}a_c}{4\pi}\sqrt{n^2 + m^2 - nm}$$

a_c = 3.70- 3.85 Å

Pt nanotubes

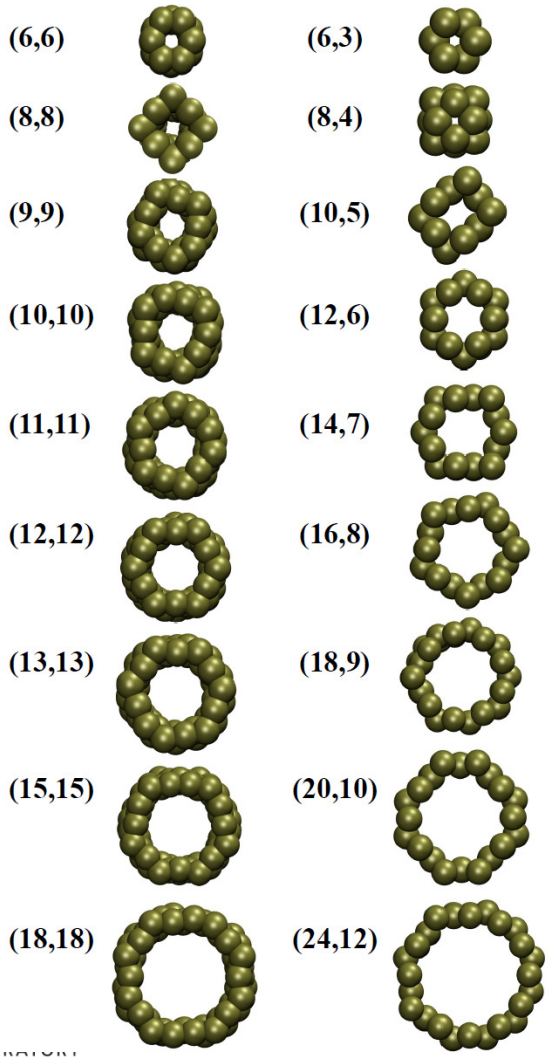

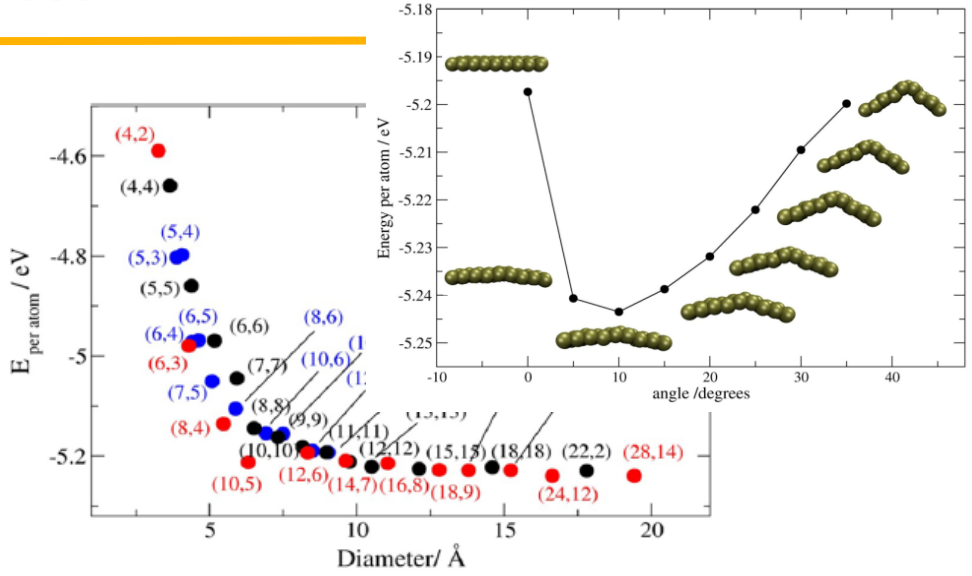

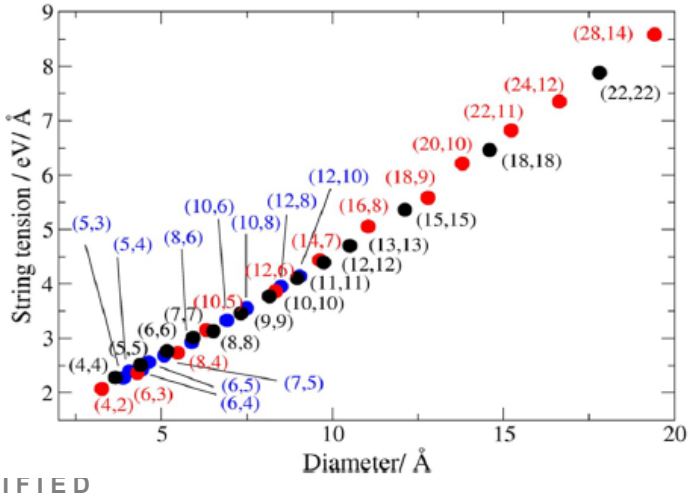

Pt nanotubes + oxygen

Adsorption energies in eV and a shift in equilibrium adsorption potential in V for oxygen on the fcc site for different nanotubes and coverages

		0.25 ML		0.33 ML		0.5 ML	
diameter		E_{ad}	ΔU_f	E_{ad}	ΔU_f	E_{ad}	ΔU_f
	Pt	−4.42	0.00	−4.25	0.00	−4.07	0.00
~0.5 nm	(6,3)	−4.72	−0.15	−4.52	−0.14	−4.50	−0.22
	(6,4)	−4.70	−0.14	−4.31	−0.03	−4.44	−0.19
	(6,6)	−4.72	−0.15	−4.41	−0.08	−4.46	−0.20
~1 nm	(12,6)	−4.29	+0.07	−3.98	+0.14	−3.96	+0.06
	(12,8)	−4.29	+0.07	−4.03	+0.11	−4.00	+0.04
	(12,12)	−4.18	+0.12	−3.94	+0.16	−3.97	+0.05
	(13,13)	−4.14	+0.14	−3.90	+0.17	−3.92	+0.08
~1 nm	(6,6)@(13,13)	−4.05	+0.19	−4.21	+0.02	−4.06	+0.01
	(5,5)@(12,12)	−4.15	+0.14	−3.94	+0.16	−4.02	+0.03

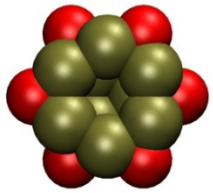

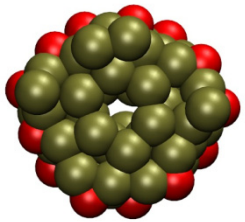

Pt nanotubes + hydroxyl

Adsorption energies in eV and a shift in equilibrium adsorption potential in V for hydroxyl on the atop site for different nanotubes and coverages

		0.25 ML		0.33 ML		0.5 ML	
diameter		E_{ad}	ΔU_f	E_{ad}	ΔU_f	E_{ad}	ΔU_f
	Pt	−2.88	0.00	−2.92	0.00	−3.09	0.00
~0.5 nm	(6,3)	−3.70	−0.82	−3.47	−0.55	−3.76	−0.67
	(6,4)	−3.60	−0.72	−3.35	−0.43	−3.69	−0.60
	(6,6)	−3.54	−0.66	−3.54	−0.62	−3.52	−0.43
~1 nm	(12,6)	−2.92	−0.04	−2.98	−0.06	−2.73	+0.36
	(12,8)	−2.89	−0.01	−2.98	−0.06	−2.84	+0.25
	(12,12)	−2.89	−0.01	−2.97	−0.05	−2.91	+0.18
	(13,13)	−2.83	+0.05	−2.87	+0.05	−2.85	+0.24
~1 nm	(6,6)@(13,13)	−3.07	−0.19	−3.13	−0.21	−3.20	−0.11
	(5,5)@(12,12)	−3.09	−0.21	−3.23	−0.31	−3.10	−0.01

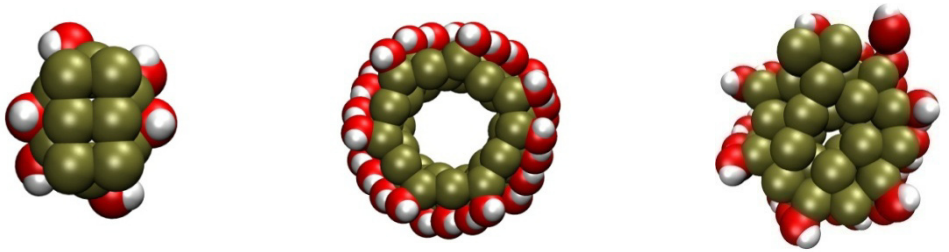

Pt nanotubes phase diagram

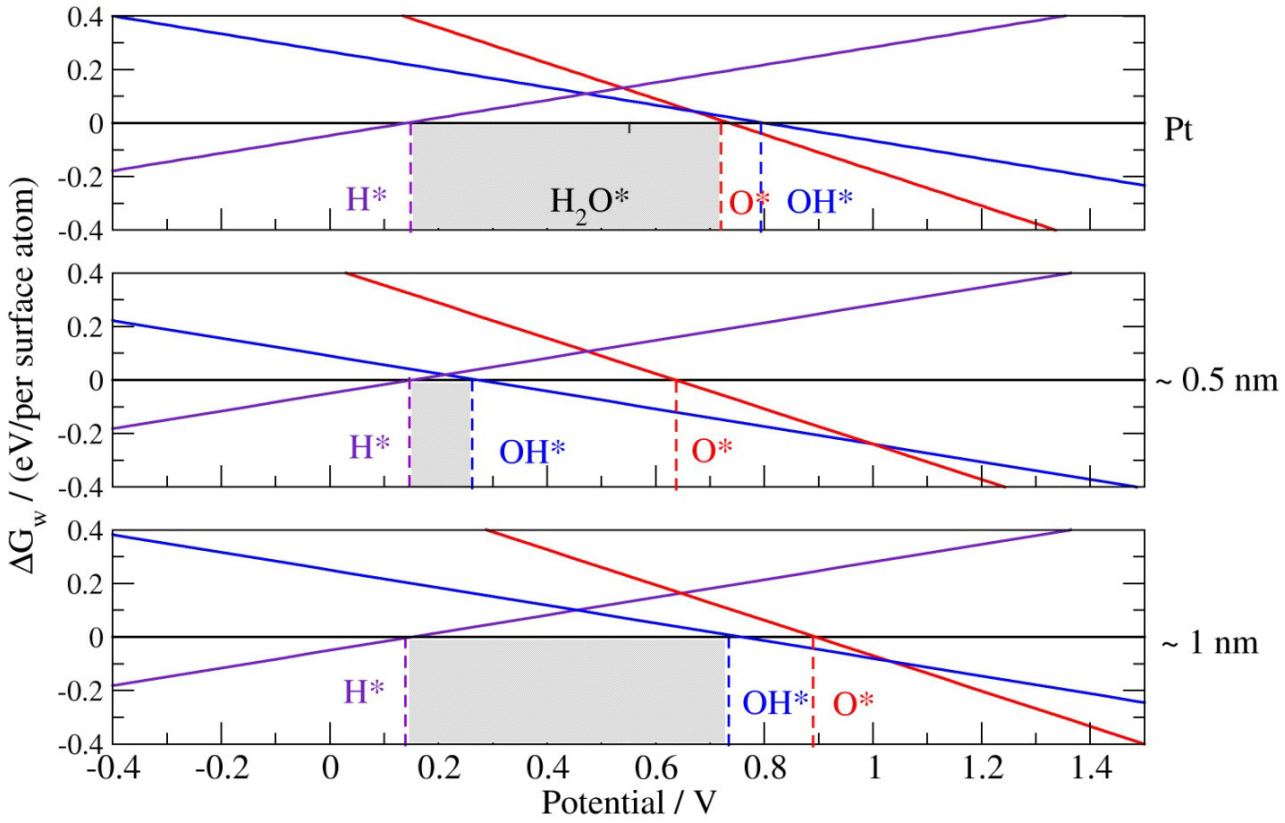

Dissociative oxygen reduction reaction (ORR) mechanism

$$\frac{1}{2}O_2 + * \rightarrow O*$$

$$O* + e^- + H^+ \rightarrow OH*$$

$$OH* + e^- + H^+ \rightarrow * + H_2O(l)$$

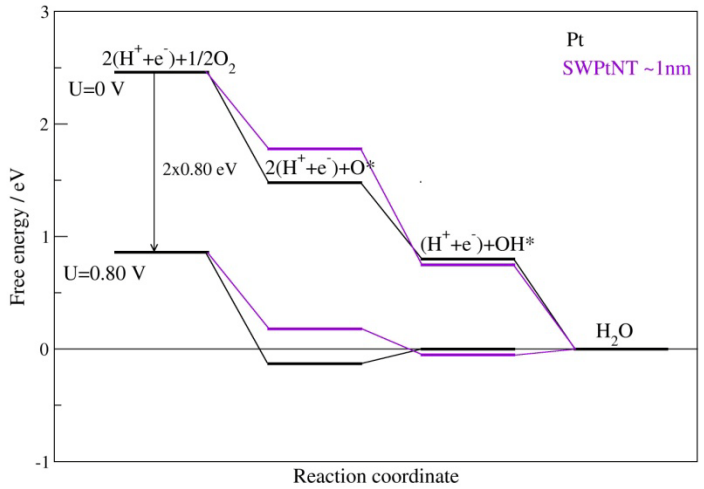

Figure: Free-energy diagrams for ORR over Pt(111) surfaces and SWPtNT for cell potentials U=0.80 V

PtNTs, d ~ 1nm

smaller ORR overpotential than Pt(111), up to 100 meV

Dissociative oxygen reduction reaction (ORR) mechanism

$$\frac{1}{2}O_2 + * \rightarrow O*$$

$$O* + e^- + H^+ \rightarrow OH*$$

$$OH* + e^- + H^+ \rightarrow * + H_2O\,(l)$$

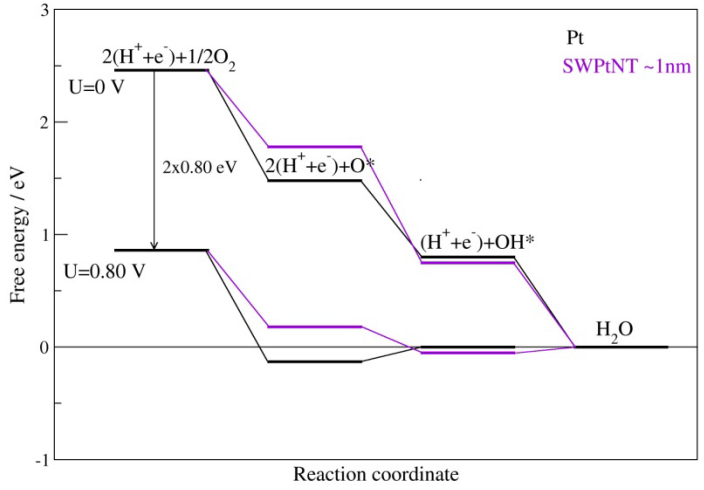

Figure: Free-energy diagrams for ORR over Pt(111) surfaces and SWPtNT for cell potentials U=0.80 V

C. Koenigsmann et al., Nano Lett., 2010, 10, 2806 – acid treated ultrathin platinum nanowires with d ~ 1nm

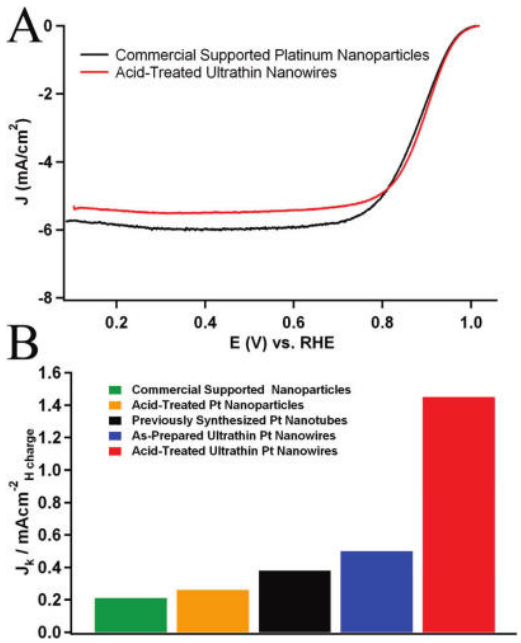

Platinum nanowires

Adsorption energies in eV for oxygen and hydroxyl for some nanotubes and nanowires

system	oxygen			hydroxyl		
	0.25 ML E_{ad}/eV	0.33 ML E_{ad}/eV	0.5 ML E_{ad}/eV	0.25 ML E_{ad}/eV	0.33 ML E_{ad}/eV	0.5 ML E_{ad}/eV
Pt	-4.42	-4.25	-4.07	-2.88	-2.92	-3.09
(6,6)NT	-4.72	-4.41	-4.46	-3.54	-3.53	-3.52
(6,6)NW	-4.62	-4.38	-4.33	-3.30	-3.42	-3.36
(13,13)NT	-4.14	-3.90	-3.92	-2.83	-2.87	-2.85
(6,6)@(13,13)NT	-4.05	-4.21	-4.06	-3.07	-3.13	-3.20
(6,6)@(13,13)NW	-4.15	-4.02	-3.97	-3.13	-3.16	-3.14

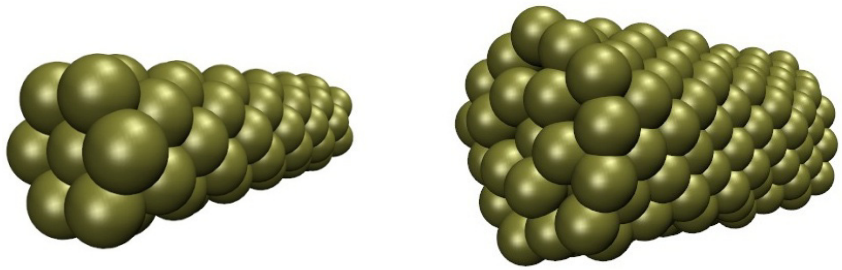

Density of states

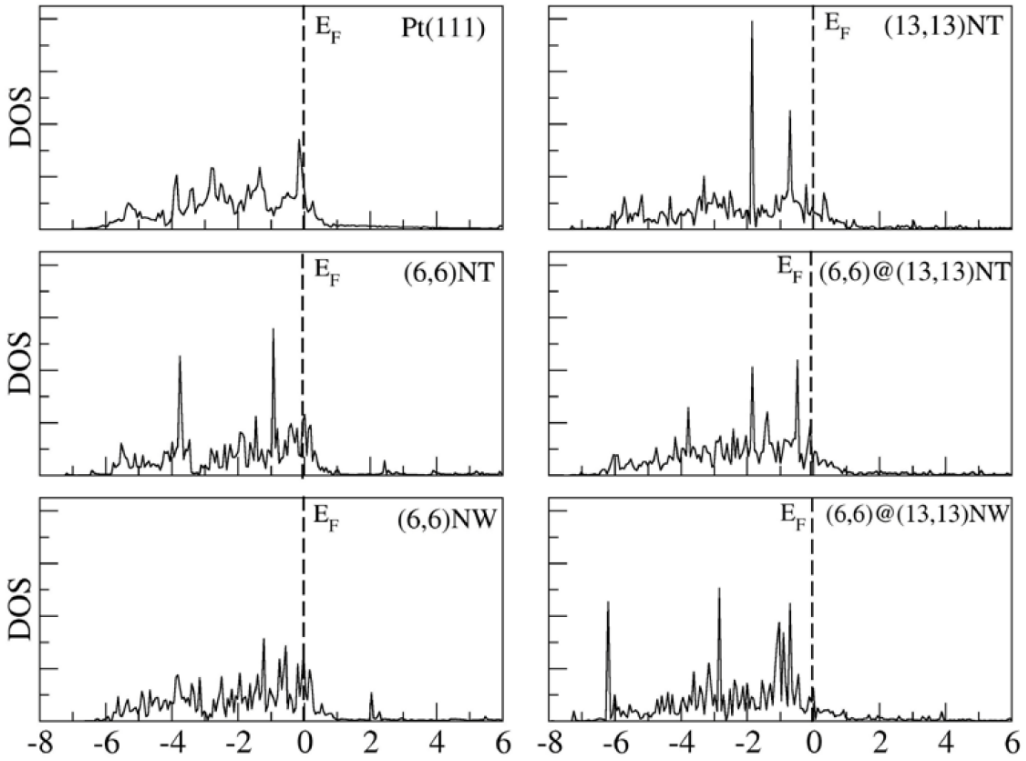

- no correlation between the position of the center of the *d*-band and the oxygen/hydroxyl adsorption energies –

effect of local environment of the adsorption site

Stability of the nanostructures

What about the stability of these nanostructures?

Electrochemical dissolution can severely decrease the performance of the material

Electrochemical dissolution

Estimate of the shift in the electrochemical dissolution potential

$$M_N(\text{surface}) \rightarrow M_{N-1} + M$$

Table: surface cohesive energy of different tubes and the shift in the electrochemical dissolution potential relative to Pt(111)

reaction: $M_N(\text{tube}) \rightarrow M_{N-1} + M$			
		ΔE (eV)	ΔU_{corr} (V)
	Pt(111)	6.50	0.00
~0.5 nm	(6,3)	3.63	−1.44
	(6,4)	5.16	−0.67
	(6,6)	5.27	−0.62
~1 nm	(12,6)	5.71	−0.40
	(12,8)	5.25	−0.63
	(12,12)	6.05	−0.23
	(13,13)	6.29	−0.11
~1 nm	(6,6)@(13,13)	5.50	−0.50
	(5,5)@(12,12)	5.67	−0.42

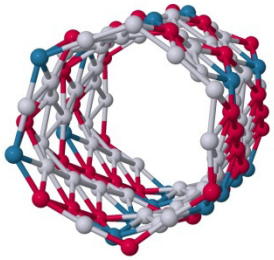

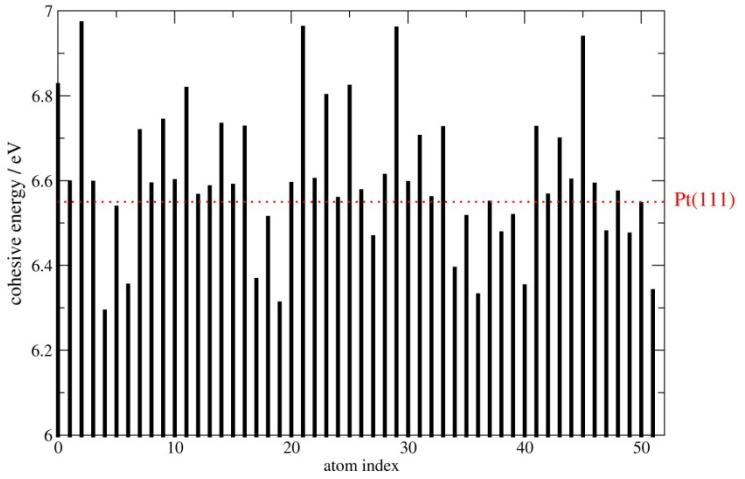

Figure. Surface cohesive energy of atoms in (13,13) tube

Pourbaix diagrams

Calculated surface Pourbaix diagrams for Pt nanotubes compared to a bulk Pourbaix diagrams (black dashed lines)

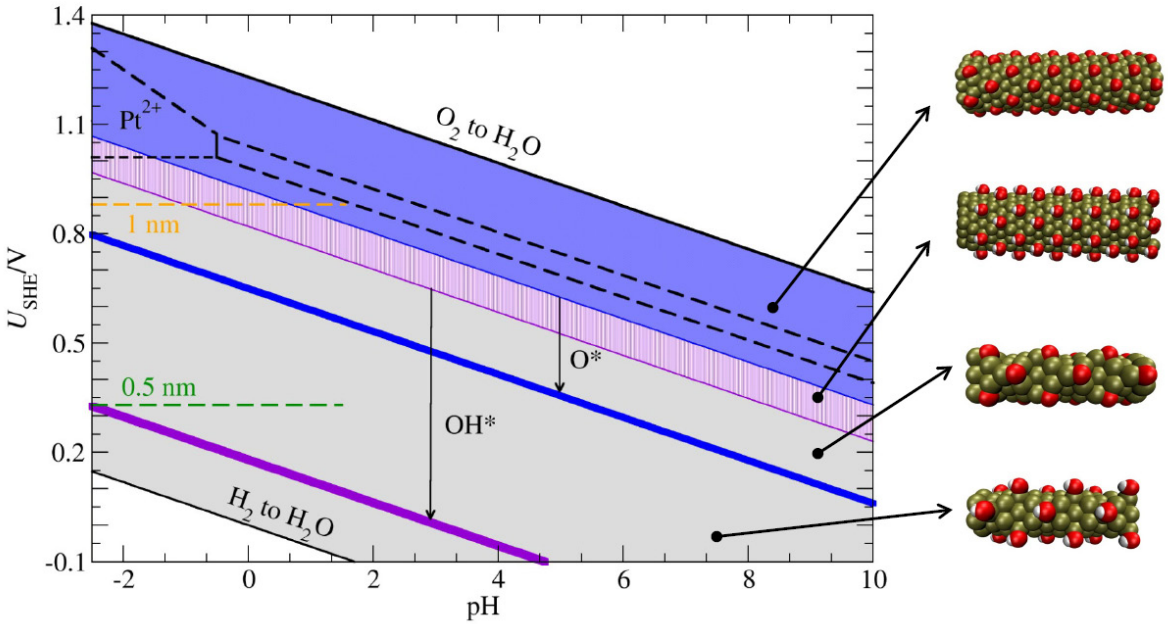

ab initio MD simulations in water

characterize change of atomic and electronic structure on solvation
structure of water around curved surfaces - water-surface interface models

(6,6) and

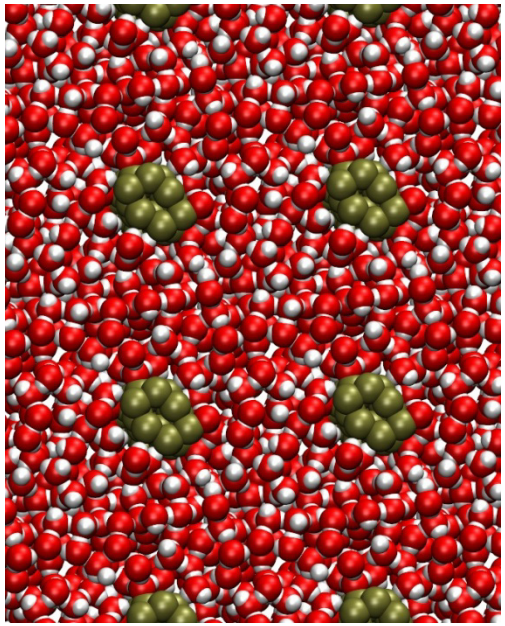

(13,13) SWPtNT in water

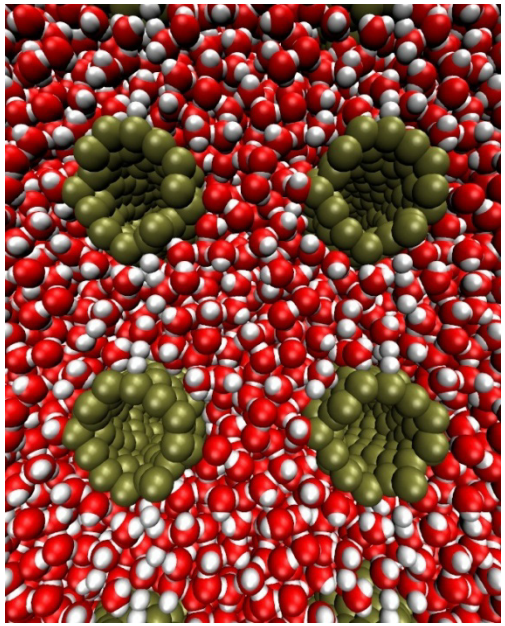

~800 atom cell, 1300 MD steps in 24h, 480 processors, average ~1min/step

- small nanotubes in water collapse to non-hollow structures, larger nanotubes stable - gas phase structure remains

ab initio MD simulations in water

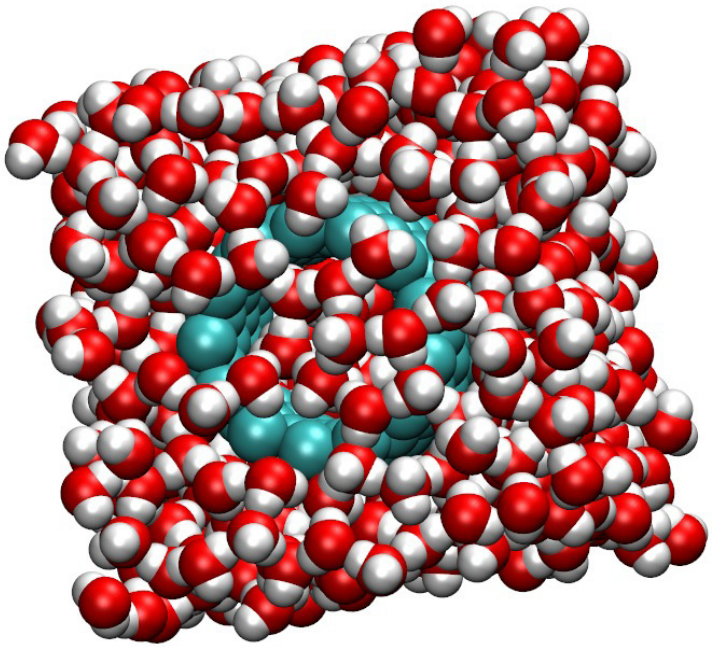

20 Å length tube, d=10.9 Å in a 30 Å length simulation box

bigger tubes accommodate water and ORR intermediates

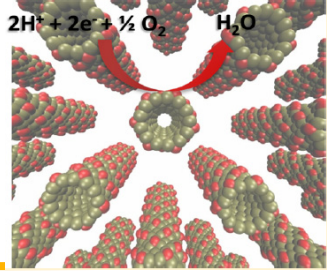

Conclusions

- smaller nanotubes (~0.5 nm) bind oxygen/hydroxyl more strongly than Pt

  larger nanotubes (~1 nm) bind oxygen/hydroxyl comparable or weaker than Pt

  reduced ORR overpotential – NT and NWs with diameter > 1nm

- control size/chirality – fine tuning of reactivity → separation of metal nanotubes by geometric specification or size

- potential corrosion problem - all studied nanotubes more susceptible to electrochemical dissolution than Pt - key property of NWs determining the critical thickness with dissolution potential lower than Pt

Acknowledgements

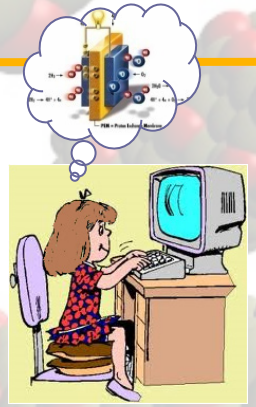

Thank you for you attention

For $$$

LANL LDRD program for postdoctoral fellowship
U.S. Department of Energy, Energy Efficiency and Renewable Energy
for financial support

for computational resources:

National Energy Research Scientific Computer Center, Pacific Northwest National Laboratory Advanced Computing Center and Center for Nanophase Materials Science

C. Taylor, J. Rossmeisl, P. Lazic

Methodology - study of ORR mechanism

Reactions connecting different states of the metal surface(*) in the ORR mechanism

$$\frac{1}{2}O_2 + * \rightarrow O*$$

$$O* + e^- + H^+ \rightarrow OH*$$

$$OH* + e^- + H^+ \rightarrow * + H_2O(l)$$

relative to the standard hydrogen electrode

$e^- + H^+(aq) = 1/2H_2(g)$

Free gibbs energy of the reactions (Norskov et al. J. Phys. Chem. B 2006, 110, 21833)

$$\Delta G_{w,water} = \Delta E_{w,water} + \Delta ZPE + T\Delta S$$

$$\Delta G(U, pH, T = 298K) = \Delta G_{w,water} \underbrace{- eU}_{\text{bias effect}} + \underbrace{kT \ln(10) pH}_{\text{correction for the free energy of H+}}$$

carbon nanotubes, 90’

AFM probe tips

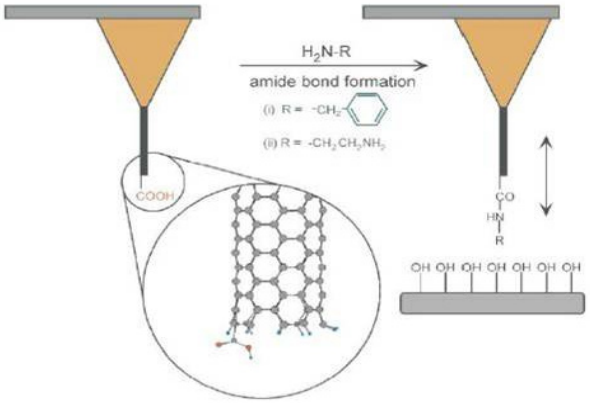

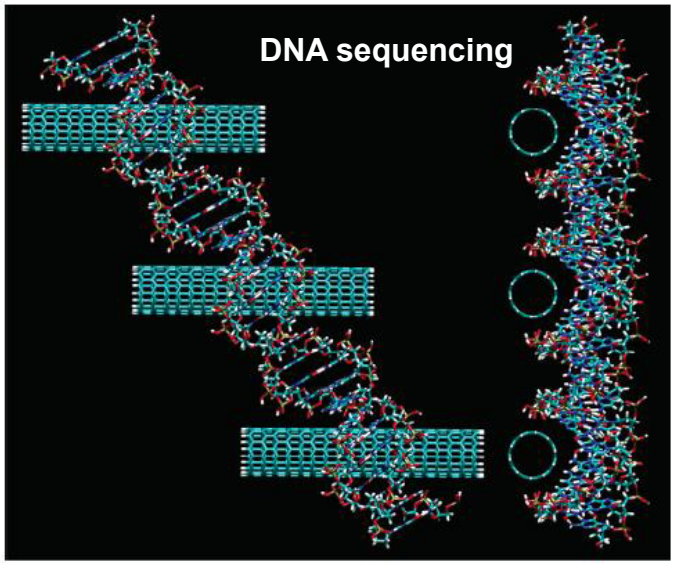

(bio)sensing, imaging, nanoelectronics

Electrochemical dissolution

Estimate of the shift in the electrochemical dissolution potential

$$M_N(\text{surface}) \rightarrow M_{N-1} + M$$

Table: surface cohesive energy of different tubes and the shift in the electrochemical dissolution potential relative to Pt(111)

reaction: $M_N(\text{tube}) \rightarrow M_{N-1} + M$			
		ΔE (eV)	ΔU_{corr} (V)
	Pt(111)	6.50	0.00
~0.5 nm	(6,3)	3.63	−1.44
	(6,4)	5.16	−0.67
	(6,6)	5.27	−0.62
~1 nm	(12,6)	5.71	−0.40
	(12,8)	5.25	−0.63
	(12,12)	6.05	−0.23
	(13,13)	6.29	−0.11
~1 nm	(6,6)@(13,13)	5.50	−0.50
	(5,5)@(12,12)	5.67	−0.42

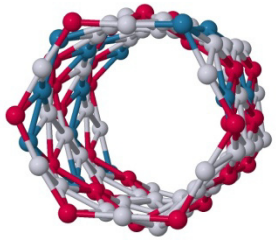

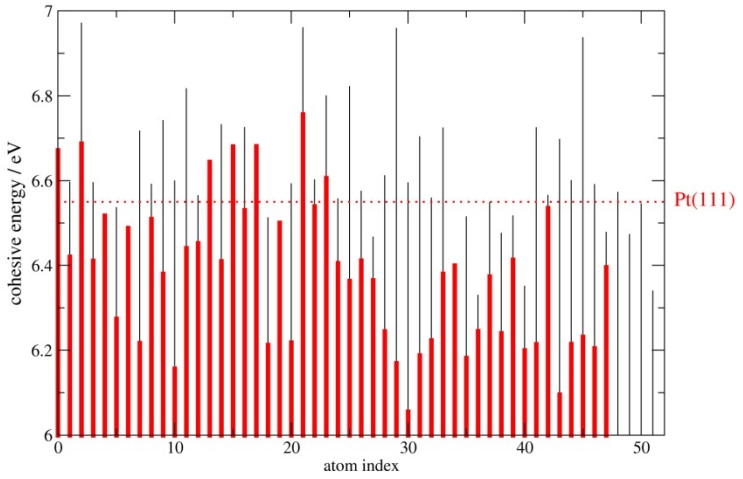

Figure. Surface cohesive energy of atoms in (12,12) tube